

Research Article

Comparative Analysis of the Time-Fractional Black–Scholes Option Pricing Equations (BSOPE) by the Laplace Residual Power Series Method (LRPSM)

Muhammad Imran Liaqat ¹ and Eric Okyere ²

¹National College of Business Administration & Economics, Lahore 54000, Pakistan

²Department of Mathematics and Statistics, University of Energy and Natural Resources, Sunyani, Ghana

Correspondence should be addressed to Eric Okyere; eric.okyere@uenr.edu.gh

Received 13 September 2022; Revised 12 October 2022; Accepted 25 November 2022; Published 16 February 2023

Academic Editor: Watcharaporn Cholamjiak

Copyright © 2023 Muhammad Imran Liaqat and Eric Okyere. This is an open access article distributed under the Creative Commons Attribution License, which permits unrestricted use, distribution, and reproduction in any medium, provided the original work is properly cited.

The residual power series method is effective for obtaining solutions to fractional-order differential equations. However, the procedure needs the $(n - 1)\omega$ derivative of the residual function. We are all aware of the difficulty of computing the fractional derivative of a function. In this article, we considered the simple and efficient method known as the Laplace residual power series method (LRPSM) to find the analytical approximate and exact solutions of the time-fractional Black–Scholes option pricing equations (BSOPE) in the sense of the Caputo derivative. This approach combines the Laplace transform and the residual power series method. The suggested method just needs the idea of an infinite limit, so the computations required to determine the coefficients are minimal. The obtained results are compared in the sense of absolute errors against those of other approaches, such as the homotopy perturbation method, the Aboodh transform decomposition method, and the projected differential transform method. The results obtained using the provided method show strong agreement with different series solution methods, demonstrating that the suggested method is a suitable alternative tool to the methods based on He's or Adomian polynomials.

1. Introduction

Fractional calculus (FC) deals with fractional derivatives and integrations. The pioneers of FC were two mathematicians, Leibniz and L'Hospital, and the date September 30, 1695, is regarded as its exact birthday. Many scientists and researchers have been drawn to FC in recent decades because it is commonly used in scientific contexts such as engineering, image processing, physics, biochemistry, biology, fluid mechanics, and entropy theory [1–5]. Although fractional derivatives can be defined in a variety of ways, not all of them are generally used. The Atangana–Baleanu, Riemann–Liouville (R-L), Caputo–Fabrizio, Caputo, and conformable operators are the most frequently used [6–12]. In some cases, fractional derivatives are preferable to integer-order derivatives for modeling because they can simulate and analyze complicated systems having complicated

nonlinear processes and higher-order behaviors. There are two main causes of this. First, we can select any order for the derivative operator, rather than being restricted to an integer order. Second, depending on both the past and current circumstances, noninteger order derivatives are advantageous when the system has long-term memory. The primary components of FC, which is the generalized version of classical calculus and has piqued the interest of numerous academics and scientists due to its wide range of applications, are fractional order differential equations (FODEs). The FODEs are frequently used for their logical support in the mathematical framework of physical problems, including technology, healthcare, monetary markets, and decision theory. As a result, the solutions provided by the FODEs are significant and useful. Applications regularly face FODEs that are too complex for close-form solutions. Under the specified initial and boundary conditions, numerical

methods present a potent alternative tool for solving FODEs. Several numerical techniques, including the Shehu decomposition approach [13], the differential transform method [14], the variational iteration method [15], the operational matrix approach [16], the homotopy analysis technique [17], the Aboodh transform decomposition method [18], the finite difference method [19], the fractional power series method [20], the Chebyshev polynomials method [21], the residual power series method [22], and the natural transform homotopy perturbation method [23], have been developed in recent years for solving FODEs.

It is efficient to obtain approximate analytical solutions to FODEs using the residual power series method (RPSM). However, the algorithm requires the $(n - 1)\omega$ derivative of the residual function. We are all aware of how difficult it is to calculate a function's fractional derivative. As a result, the use of conventional RPSM is somewhat constrained. To overcome the limitations of the RPSM, Eriqat et al. introduced a new technique called LRPSM [24]. Several FODEs have been solved through the recommended method [24–29]. The provided equation is transformed into the Laplace transform (LT) space in accordance with the set of rules for this novel approach; the solution to the new form of the problem is established; the solution to the original equation is then achieved by applying the inverse LT.

The pricing of financial derivatives is a topic that has generated a great deal of interest and literature. A financial derivative is an asset whose price is based on the value of another asset. Frequently, a stock or bond serves as the

underlying asset. Financial derivatives are not a completely novel concept. It is generally agreed that Charles Castelly's work, which was published in 1877, was the first attempt at contemporary derivative pricing, despite some historical controversy regarding the exact year of the birth of financial derivatives [30]. Although it lacked mathematical rigor, Castell's book served as a general introduction to ideas such as hedging and speculative trading.

The first widely used mathematical method to calculate the theoretical value of an option contract using prevailing equity markets' predicted dividends, the option's strike price, projected interest rates, time till the cessation, and expected unpredictability was the Black–Scholes (BS) model, developed in 1997 by Fischer Black, Robert Merton, and Myron Scholes. The Pricing of Options and Corporate Liabilities by Black and Scholes, published in the Journal of Political Economy in 1973, provided the initial formulation of the equation. Robert C. Merton contributed to the editing of that document. Later that year, he wrote his own work, "Theory of Rational Option Pricing," expanding the model's mathematical capabilities and applications while also coining the term "BS theory of options pricing" [31]. One of the most significant mathematical representations of a financial market is the BS equation. The value of financial derivatives is controlled by a second-order parabolic partial differential equation. Many different commodities and payout structures have been used in the BS model for pricing stock options. The following equation describes the BS model for the value of an option [32]:

$$\frac{\partial^\omega w(\kappa, \zeta)}{\partial \zeta^\omega} + \frac{\sigma^2 \kappa^2}{2} \frac{\partial^2 w(\kappa, \zeta)}{\partial \kappa^2} + \mathfrak{F}(\zeta) \kappa \frac{\partial w(\kappa, \zeta)}{\partial \kappa} - \mathfrak{F}(\zeta) w(\kappa, \zeta) = 0, \quad (1)$$

where ω is the order of the Caputo derivative (CD), $w(\kappa, \zeta)$ is the European offer's value at the fundamental market cap of κ and time ζ , the fluctuation component of the company's shares, often referred to as σ , quantifies the variance of the stock's return, Y is the expiration date, and $\mathfrak{F}(\zeta)$ is the risk-free interest rate. $w_c(\kappa, \zeta)$ and $w_p(\kappa, \zeta)$, correspondingly, stand for the call and put values on European options. Then, the payoff functions are given by $w_c(\kappa, \zeta) = \max(\kappa - U, 0)$ and $w_p(\kappa, \zeta) = \max(U - \kappa, 0)$, where U indicates the termination price for the option and the function $\max(\kappa, 0)$ gives the larger value between κ and 0. The important financial view of the BS equation is that it minimizes risk by allowing for the prudent selection of purchasing and selling the stock under scrutiny. It is a sign that, according to the BS financial model, there is only one correct price for the option. The important financial view of the BS equation is that it minimizes risk by allowing for the prudent selection of purchasing and selling the stock under scrutiny. It is a sign that, according to the BS financial model, there is only one correct price for the option. In this article, a fractional model that may be used to model the pricing of various financial derivatives is presented.

Numerous techniques have been used to examine the time-fractional BSOPE [33–40]. Each of these techniques has specific restrictions and flaws. These techniques involve a lot of computing work and a long running time. In this article, we considered LRPSM, which is a simple and efficient technique to solve BSOPE. The advantage of the recommended method over the homotopy perturbation method (HPM) and the Adomian decomposition method (ADM) is its strength in handling problems without the use of He's and Adomian polynomials. The advantage of this approach is that the problem does not involve any physical parameter assumptions, no matter how big or small. For a series such as the RPSM, the coefficients must be determined each time using the fractional derivative. Since LRPSM just needs the idea of an infinite limit, the computations required to determine the coefficients are minimal. The LRPSM results are also compared to those of other approaches, including the projected differential transform method (PDTM) [34], the Aboodh transform decomposition method (ATMD) [35], and the homotopy perturbation method (HPM) [36]. The results obtained using the suggested method show strong agreement with numerous methodologies, proving that the

LRPSM is a useful substitute for approaches using He’s or Adomian polynomials. Additionally, error functions are used to compare the exact and approximative solutions graphically and numerically. The higher degrees of accuracy and convergence rates were confirmed by the error analysis, demonstrating the suggested method’s efficacy and reliability. The process is rapid, exact, and simple to use, and it produces excellent results.

The article’s structure is as follows: In Section 2, we use a number of important definitions and conclusions from the theory of FC. The main concept of LRPSM is examined in Section 3 in order to establish and determine the solution of the time-fractional BSOPE. Section 4 investigates the potential, capability, and simplicity of the suggested approach using three numerical models. In Section 5, graphics and tables are used to investigate the numerical outcomes and discussion. Section 6, towards the end, has the conclusion.

2. Preliminaries

In this section, we examine several common definitions, properties, and some useful consequences that we used in this article.

Definition 1 (see [24]). We assume that the function $w(x, \zeta)$ is of exponential order δ and piecewise continuous. Then, the LT of $w(x, \zeta)$ for $\zeta \geq 0$ is formulated as

$$\mathcal{L}[w(x, \zeta)] = W(x, s) = \int_0^\infty w(x, \zeta)e^{-s\zeta}d\zeta, \quad s > \delta, \quad (2)$$

and the inverse LT is defined by

$$\mathcal{L}^{-1}[W(x, s)] = w(x, \zeta) = \int_{h-\infty}^{h+\infty} e^{s\zeta}W(x, s)ds, \quad h = \text{Re}(s) > h_0, \quad (3)$$

where h_0 lies in the right half plane of the absolute convergence of the Laplace integral.

Lemma 1 (see [24–29]). Let $w_1(x, \zeta)$ and $w_2(x, \zeta)$ be piecewise continuous on $[0, \infty$ and be of exponential order. We assume that $\mathcal{L}[w_1(x, \zeta)] = W_1(x, s)$, $\mathcal{L}[w_2(x, \zeta)] = W_2(x, s)$, and c_1, c_2 are constants. Then, the properties mentioned as follows are valid:

- (i) $\mathcal{L}[c_1w_1(x, \zeta) + c_2w_2(x, \zeta)] = c_1W_1(x, s) + c_2W_2(x, s)$
- (ii) $\mathcal{L}^{-1}[c_1W_1(x, s) + c_2W_2(x, s)] = c_1w_1(x, \zeta) + c_2w_2(x, \zeta)$
- (iii) $\phi_0(x) = \lim_{s \rightarrow \infty} sW(x, s) = w(x, 0)$

- (iv) $\mathcal{L}[D_\zeta^\omega w(x, \zeta)] = s^\omega W(x, s) - \sum_{j=0}^{n-1} w^{(j)}(x, 0)/s^{j-\omega+1}, n-1 < \omega \leq n, n \in \mathbb{N}$
- (v) $\mathcal{L}[D_\zeta^{n\omega} w(x, \zeta)] = s^{n\omega} W(x, s) - \sum_{j=0}^{n-1} s^{\omega(n-j)-1} D_\zeta^{j\omega} w(x, 0), 0 < \omega \leq 1$

Definition 2 (see [41]). The fractional derivative of $w(x, \zeta)$ I order ω in the CD sense is defined as follows:

$$D_\zeta^\omega w(x, \zeta) = \mathcal{I}_\zeta^{n-\omega} w^{(n)}(x, \zeta), \quad \zeta \geq 0, \quad n-1 < \omega \leq n, \quad (4)$$

where $\mathcal{I}_\zeta^{n-\omega}$ is the R-L integral of $w(x, \zeta)$.

Theorem 1 (see [24]). We assume that the multiple fractional power series (MFPS) representation for the function $\mathcal{L}[w(x, \zeta)] = W(x, s)$ is given by

$$W(x, s) = \sum_{n=0}^\infty \frac{\phi_n(x)}{s^{n\omega+1}}, \quad s > 0, \quad (5)$$

then we have

$$\phi_n(x) = D_\zeta^{n\omega} w(x, 0), \quad (6)$$

where $D_\zeta^{n\omega} = D_\zeta^\omega \cdot D_\zeta^\omega \dots D_\zeta^\omega$ (n – times).

The conditions for the convergence of the MFPS are determined in the following theorem.

Theorem 2 (see [24]). Let $\mathcal{L}[w(x, \zeta)] = W(x, s)$ can be denoted as the new form of MFPS explained in Theorem 1. If $|\mathcal{L}[D_\zeta^{(j+1)\omega} w(x, \zeta)]| \leq \mathcal{L}$, on $0 < s \leq v$ with $0 < \omega \leq 1$, then the remainder $R_j(x, s)$ of the new form of MFPS satisfies the following inequality:

$$|R_j(x, s)| \leq \frac{\mathcal{L}}{s^{(j+1)\omega+1}}, \quad 0 < s \leq v. \quad (7)$$

3. Methodology for the LRPSM for the Time-Fractional BSOPE

This section examines the steps for using the suggested method to find solutions to BSOPEs. Running the LT on the BSOPE and then considering MFPS as the BSOPE’s new space solution constitute the main idea of LRPSM. The way in which the coefficients of this series utilize the limit idea is the main difference between the LRPSM and the RPSM. The generated consequents are then transformed into real space using the inverse LT. The guidelines for using the LRPSM to find solutions are as follows:

Step 1: Equation (1) should be changed as follows:

$$D_\zeta^\omega w(x, \zeta) - f\left(w(x, \zeta), \frac{\sigma^2 x^2 \partial^2 w(x, \zeta)}{2\partial x^2}, \mathfrak{F}(\zeta)x \frac{\partial w(x, \zeta)}{\partial x}, \mathfrak{F}(\zeta)w(x, \zeta)\right) = 0. \quad (8)$$

Step 2: by considering LT on both sides of equation (8), we obtain the following:

$$W(x, s) - \frac{w(x, 0)}{s} - \frac{1}{s^\omega} F(x, s) = 0, \quad (9)$$

where

$$W(\kappa, s) = \mathcal{L}[w(\kappa, \zeta)], \quad (10)$$

and

$$F(\kappa, s) = \mathcal{L}\left[f\left(\frac{\sigma^2 \kappa^2 \partial^2 w(\kappa, \zeta)}{2\partial \kappa^2}, \mathfrak{F}(\zeta)w(\kappa, \zeta), w(\kappa, \zeta), \mathfrak{F}(\zeta)\kappa \frac{\partial w(\kappa, \zeta)}{\partial \kappa}\right)\right]. \quad (11)$$

Step 3: we assume that the solution of equation (9) is the following series:

$$W(\kappa, s) = \sum_{n=0}^{\infty} \frac{\phi_n(\kappa)}{s^{m\kappa+1}}, \quad s > 0. \quad (12)$$

Step 4: we obtained the following as a result of using Lemma 1(iii):

$$\phi_0(\kappa) = \lim_{s \rightarrow \infty} sW(\kappa, s) = w(\kappa, 0) = 0. \quad (13)$$

Step 5: we define the k th-truncated expansion of $W(\kappa, s)$ as

$$W_k(\kappa, s) = \frac{\phi_0(\kappa)}{s} + \sum_{n=1}^k \frac{\phi_n(\kappa)}{s^{n\omega+1}}. \quad (14)$$

Step 6: we introduce Laplace residual function (LRF) of equation (9) and the k th-LRF, respectively, as follows:

$$\mathcal{L}[\text{Res}(\kappa, s)] = W(\kappa, s) - \frac{\phi_0(\kappa)}{s} - \frac{1}{s^\omega} F(s), \quad (15)$$

$$\mathcal{L}[\text{Res}_k(\kappa, s)] = W_k(\kappa, s) - \frac{\phi_0(\kappa)}{s} - \frac{1}{s^\omega} F_k(s). \quad (16)$$

Step 7: we use the expansion form of $W_k(\kappa, s)$ into $\mathcal{L}[\text{Res}_k(\kappa, s)]$.

Step 8: we multiply both sides of $\mathcal{L}[\text{Res}_k(\kappa, s)]$ with $s^{k\omega+1}$.

Step 9: by utilizing the fact in equation (16), we solve the following sequence of algebraic equations for $\phi_n(\kappa)$, where $n = 1, 2, 3, \dots, k$, step by step:

$$\lim_{s \rightarrow \infty} (s^{\omega+1} \mathcal{L}[\text{Res}_k(\kappa, s)]) = 0, \quad k = 1, 2, 3, \dots \quad (17)$$

Step 10: we use the attained values of $\phi_n(\kappa)$ into the k th-truncated expansion of $W(\kappa, s)$ for each $n = 1, 2, 3, \dots, k$ to attain the k th-approximate solution of the algebraic equation in equation (9).

Step 11: we apply the inverse LT on the final form of $W_k(\kappa, s)$ to attain k th-approximate solution, $w_k(\kappa, \zeta)$ of the suggested problem.

4. Some Illustrated Problems

In this section, three time-fractional BSOPE in the CD sense are solved in order to assess the effectiveness and suitability of the suggested approach.

Problem 1. consider the time-fractional BSOPE that follows [34]:

$$\frac{\partial^\omega w(\kappa, \zeta)}{\partial \zeta^\omega} + \kappa^2 \frac{\partial^2 w(\kappa, \zeta)}{\partial \kappa^2} + 0.5\kappa \frac{\partial w(\kappa, \zeta)}{\partial \kappa} - w(\kappa, \zeta) \quad (18)$$

$$= 0, \quad 0 < \omega \leq 1,$$

under the following initial conditions:

$$w(\kappa, 0) = \max(\kappa^3, 0) = \begin{cases} \kappa^3 & \text{for } \kappa > 0, \\ 0 & \text{for } \kappa \leq 0. \end{cases} \quad (19)$$

We will examine the case when $\kappa > 0$. Applying LT on both sides of equation (18), we have

$$\mathcal{L}\left[\frac{\partial^\omega w(\kappa, \zeta)}{\partial \zeta^\omega} + \kappa^2 \frac{\partial^2 w(\kappa, \zeta)}{\partial \kappa^2} + 0.5\kappa \frac{\partial w(\kappa, \zeta)}{\partial \kappa} - w(\kappa, \zeta)\right] = 0. \quad (20)$$

Making use of the process outlined in Section 3, we get the findings from equation (20) as follows:

$$W(\kappa, s) = \frac{\kappa^3}{s} - \frac{1}{s^\omega} \kappa^2 D_{\kappa\kappa} \mathcal{L}[w(\kappa, \zeta)] - \frac{1}{s^\omega} 0.5\kappa D_\kappa \mathcal{L}[w(\kappa, \zeta)] + \frac{1}{s^\omega} \mathcal{L}[w(\kappa, \zeta)]. \quad (21)$$

We suppose that the expansion of $W(\kappa, s)$ is as follows:

$$W(\chi, s) = \sum_{n=0}^{\infty} \frac{\phi_n(\chi)}{s^{n\omega+1}}. \tag{22}$$

The k th-truncated expansion is given as follows:

$$W_k(\chi, s) = \sum_{n=0}^k \frac{\phi_n(\chi)}{s^{n\omega+1}}. \tag{23}$$

We obtained the following as a result of using Lemma 1(iii):

$$\mathcal{L}[\text{Res}(\chi, s)] = W(\chi, s) - \frac{\chi^3}{s} + \frac{1}{s^\omega} \chi^2 D_{\chi\chi} W(\chi, s) + \frac{1}{s^\omega} (0.5) \chi D_\chi W(\chi, s) - \frac{1}{s^\omega} W(\chi, s). \tag{26}$$

The k th-LRF of equation (21) is as follows:

$$\mathcal{L}[\text{Res}_k(\chi, s)] = W_k(\chi, s) - \frac{\chi^3}{s} + \frac{1}{s^\omega} \chi^2 D_{\chi\chi} W_k(\chi, s) + \frac{1}{s^\omega} (0.5) \chi D_\chi W_k(\chi, s) - \frac{1}{s^\omega} W_k(\chi, s). \tag{27}$$

We expand the characteristics of the RPSM to highlight the following details [42, 43]:

- (i) $\mathcal{L}[\text{Res}(\chi, s)] = 0$ and $\lim_{s \rightarrow \infty} \mathcal{L}[\text{Res}_k(\chi, s)]$
- (ii) $\lim_{s \rightarrow \infty} s \mathcal{L}[\text{Res}(\chi, s)] = 0 \Rightarrow \lim_{s \rightarrow \infty} s \mathcal{L}[\text{Res}_k(\chi, s)]$

$$\phi_0(\chi) = \lim_{s \rightarrow \infty} sW(s) = w(\chi, 0) = \chi^3. \tag{24}$$

As a result, the k th-truncate expansion of equation (21) is as follows:

$$W_k(\chi, s) = \frac{\chi^3}{s} + \sum_{n=1}^k \frac{\phi_n(\chi)}{s^{n\omega+1}}. \tag{25}$$

The LRF of equation (21) is as follows:

- (iii) $\lim_{s \rightarrow \infty} s^{k\omega+1} \mathcal{L}[\text{Res}(\chi, s)] = \lim_{s \rightarrow \infty} s^{k\omega+1} \mathcal{L}[\text{Res}_k(\chi, s)] \stackrel{s \rightarrow \infty}{=} 0$, where $k = 1, 2, 3, \dots$. To determine the first unknown co-efficient $\phi_1(\chi)$ in (25), we have to use the 1st truncated series $W_1(\chi, s) = \chi^3/s + \phi_1(\chi)/s^{\omega+1}$ into the 1st-LRF, $\mathcal{L}[\text{Res}_1(\chi, s)]$, to obtain

$$\mathcal{L}[\text{Res}_1(\chi, s)] = \left[\frac{\chi^3}{s} + \frac{\phi_1(\chi)}{s^{\omega+1}} \right] - \frac{\chi^3}{s} + \frac{1}{s^\omega} \chi^2 D_{\chi\chi} \left[\frac{\chi^3}{s} + \frac{\phi_1(\chi)}{s^{\omega+1}} \right] + \frac{1}{s^\omega} (0.5) \chi D_\chi \left[\frac{\chi^3}{s} + \frac{\phi_1(\chi)}{s^{\omega+1}} \right] - \frac{1}{s^\omega} \left[\frac{\chi^3}{s} + \frac{\phi_1(\chi)}{s^{\omega+1}} \right]. \tag{28}$$

$s^{\omega+1}$ is used on both sides of equation (28):

$$s^{\omega+1} \mathcal{L}[\text{Res}_1(\chi, s)] = \phi_1(\chi) + \chi^2 D_{\chi\chi} \left[\chi^3 + \frac{\phi_1(\chi)}{s^\omega} \right] + (0.5) \chi D_\chi \left[\chi^3 + \frac{\phi_1(\chi)}{s^\omega} \right] - \left[\chi^3 + \frac{\phi_1(\chi)}{s^\omega} \right]. \tag{29}$$

We use the fact that

$$\lim_{s \rightarrow \infty} s^{k\omega+1} \mathcal{L}[\text{Res}_k(\chi, s)] = 0, \text{ for } k = 1. \tag{30}$$

As a result, we obtained as follows:

$$\phi_1(\chi) = -6.5\chi^3. \tag{31}$$

Similarly, to find out values of the second undefined coefficient $\phi_2(\chi)$, we have to use the 2nd-truncates series $W_2(\chi, s) = \chi^3/s + \phi_1(\chi)/s^{\omega+1} + \phi_2(\chi)/s^{2\omega+1}$ into the 2nd-LRF to obtain

$$\begin{aligned} \mathcal{L}[\text{Res}_2(\chi, s)] &= \left[\frac{\chi^3}{s} + \frac{\phi_1(\chi)}{s^{\omega+1}} + \frac{\phi_2(\chi)}{s^{2\omega+1}} \right] - \frac{\chi^3}{s} + \frac{1}{s^\omega} \chi^2 D_{\chi\chi} \left[\frac{\chi^3}{s} + \frac{\phi_1(\chi)}{s^{\omega+1}} + \frac{\phi_2(\chi)}{s^{2\omega+1}} \right] \\ &+ \frac{1}{s^\omega} (0.5) \chi D_\chi \left[\frac{\chi^3}{s} + \frac{\phi_1(\chi)}{s^{\omega+1}} + \frac{\phi_2(\chi)}{s^{2\omega+1}} \right] - \frac{1}{s^\omega} \left[\frac{\chi^3}{s} + \frac{\phi_1(\chi)}{s^{\omega+1}} + \frac{\phi_2(\chi)}{s^{2\omega+1}} \right]. \end{aligned} \tag{32}$$

Using $s^{2\omega+1}$ on both sides of equation (32), we get the following equation:

$$s^{2\omega+1} \mathcal{L} [\text{Res}_2(\kappa, s)] = s^\omega \phi_1(\kappa) + \phi_2(\kappa) + s^{\omega+1} \kappa^2 D_{\kappa\kappa} \left[\frac{\kappa^3}{s} + \frac{\phi_1(\kappa)}{s^{\omega+1}} + \frac{\phi_2(\kappa)}{s^{2\omega+1}} \right] + s^{\omega+1} (0.5) D_\kappa \left[\frac{\kappa^3}{s} + \frac{\phi_1(\kappa)}{s^{\omega+1}} + \frac{\phi_2(\kappa)}{s^{2\omega+1}} \right] - s^{\omega+1} \left[\frac{\kappa^3}{s} + \frac{\phi_1(\kappa)}{s^{\omega+1}} + \frac{\phi_2(\kappa)}{s^{2\omega+1}} \right]. \tag{33}$$

Again, we use the fact that

$$\lim_{s \rightarrow \infty} s^{k\omega+1} \mathcal{L} [\text{Res}_k(\kappa, s)] = 0, \text{ for } k = 2. \tag{34}$$

As a result, we obtained the 2nd coefficient $\phi_1(\kappa)$ in the following form:

$$\phi_2(\kappa) = (6.5)^2 \kappa^3. \tag{35}$$

Therefore, the 2nd-approximate LRPS solution of equation (21) is

$$W_2(\kappa, s) = \frac{1}{s} \kappa^3 - \frac{6.5}{s^{\omega+1}} \kappa^3 + \frac{(6.5)^2}{s^{2\omega+1}} \kappa^3. \tag{36}$$

Typically, to find the coefficients $\phi_k(\kappa)$, first we use the k th-truncated series in equation (25), then we utilize it in the k th-LRF, equation (27), we multiply $\mathcal{L} [\text{Res}_k(\kappa, s)]$ by $s^{k\omega+1}$, and then we solve the algebraic equation as follows:

$$\lim_{s \rightarrow \infty} s^{k\omega+1} \mathcal{L} [\text{Res}_k(\kappa, s)] = 0, \text{ for } \phi_k(\kappa). \tag{37}$$

We get the following results by utilizing the previous procedure:

$$\begin{aligned} \phi_3(\kappa) &= -(6.5)^3 \kappa^3, \\ \phi_4(\kappa) &= (6.5)^4 \kappa^3, \\ \phi_5(\kappa) &= -(6.5)^5 \kappa^3. \end{aligned} \tag{38}$$

The approximate solution of equation (21) is obtained by five iterations as follows:

$$W_5(\kappa, s) = \frac{\kappa^3}{s} - \frac{6.5\kappa^3}{s^{\omega+1}} + \frac{(6.5)^2\kappa^3}{s^{2\omega+1}} - \frac{(6.5)^3\kappa^3}{s^{3\omega+1}} + \frac{(6.5)^4\kappa^3}{s^{4\omega+1}} - \frac{(6.5)^5\kappa^3}{s^{5\omega+1}}. \tag{39}$$

By applying the inverse LT to equation (39), we are able to approximate the fifth step solution in the original feature space:

$$w_5(\kappa, \zeta) = \kappa^3 - \frac{6.5\kappa^3\zeta^\omega}{\Gamma(\omega+1)} + \frac{(6.5)^2\kappa^3\zeta^{2\omega}}{\Gamma(2\omega+1)} - \frac{(6.5)^3\kappa^3\zeta^{3\omega}}{\Gamma(3\omega+1)} + \frac{(6.5)^4\kappa^3\zeta^{4\omega}}{\Gamma(4\omega+1)} - \frac{(6.5)^5\kappa^3\zeta^{5\omega}}{\Gamma(5\omega+1)}. \tag{40}$$

When we use $\omega = 1$ in equation (40), we get the following form:

$$w_5(\kappa, \zeta) = \kappa^3 \left[1 + \frac{(-6.5\zeta)}{1!} + \frac{(-6.5\zeta)^2}{2!} + \frac{(-6.5\zeta)^3}{3!} + \frac{(-6.5\zeta)^4}{4!} + \frac{(-6.5\zeta)^5}{5!} \right], \tag{41}$$

which are the first six terms of the expansion $\kappa^3 e^{-6.5\zeta}$ and, thus, is the exact solution of equations (18) and (19) at $\omega = 1$.

Problem 2. consider the following time-fractional BSOPE [35]:

$$\frac{\partial^\omega w(\kappa, \zeta)}{\partial \zeta^\omega} + 0.08(2 + \sin \kappa)^2 \kappa^2 \frac{\partial^2 w(\kappa, \zeta)}{\partial \kappa^2} + 0.06\kappa \frac{\partial w(\kappa, \zeta)}{\partial \kappa} = 0.06w(\kappa, \zeta), \quad 0 < \omega \leq 1, \tag{42}$$

subject to the following initial conditions:

$$w(\varkappa, 0) = \max(\varkappa - 25e^{-0.06}, 0). \tag{43}$$

First, we perform LT on both sides of equation (42), we use the initial condition from equation (43), and then we format the resulting equation as follows:

$$W(\varkappa, s) = \frac{1}{s} \max(\varkappa - 25e^{-0.06}, 0) - \frac{1}{s^{\omega}} 0.08(2 + \sin \varkappa)^2 \varkappa^2 D_{\varkappa \varkappa} W(\varkappa, s) - \frac{0.06 \varkappa}{s^{\omega}} D_{\varkappa} W(\varkappa, s) + \frac{0.06}{s^{\omega}} W(\varkappa, s). \tag{44}$$

We describe the expansion solution of the algebraic equation (44). So, we suppose that the series of $W(\varkappa, s)$ is as follows:

$$W(\varkappa, s) = \sum_{n=0}^{\infty} \frac{\phi_n(\varkappa)}{s^{n\omega+1}}. \tag{45}$$

The k th-truncated series of the expansion of $W(\varkappa, s)$ is as follows:

$$W_k(\varkappa, s) = \sum_{n=0}^k \frac{\phi_n(\varkappa)}{s^{n\omega+1}}. \tag{46}$$

We obtained the following as a result of using Lemma 1(iii):

$$\phi_0(\varkappa) = \lim_{s \rightarrow \infty} sW(\varkappa, s) = w(\varkappa, 0) = \max(\varkappa - 25e^{-0.06}, 0). \tag{47}$$

So, the k th-truncated expansion becomes as follows:

$$W_k(\varkappa, s) = \frac{1}{s} \max(\varkappa - 25e^{-0.06}, 0) + \sum_{n=1}^k \frac{\phi_n(\varkappa)}{s^{n\omega+1}}. \tag{48}$$

The LRF of (44) is as follows:

$$\mathcal{L}[\text{Res}(\varkappa, s)] = W(\varkappa, s) - \frac{1}{s} \max(\varkappa - 25e^{-0.06}, 0) + \frac{1}{s^{\omega}} 0.08(2 + \sin \varkappa)^2 \varkappa^2 D_{\varkappa \varkappa} W(\varkappa, s) + \frac{0.06 \varkappa}{s^{\omega}} D_{\varkappa} W(\varkappa, s) - \frac{0.06}{s^{\omega}} W(\varkappa, s). \tag{49}$$

The k th-LRF of equation (44) is designed as follows:

$$\begin{aligned} \mathcal{L}[\text{Res}_k(\varkappa, s)] &= W_k(\varkappa, s) - \frac{1}{s} \max(\varkappa - 25e^{-0.06}, 0) + \frac{1}{s^{\omega}} 0.08(2 + \sin \varkappa)^2 \varkappa^2 D_{\varkappa \varkappa} W_k(\varkappa, s) \\ &\quad + \frac{0.06 \varkappa}{s^{\omega}} D_{\varkappa} W_k(\varkappa, s) - \frac{0.06}{s^{\omega}} W_k(\varkappa, s). \end{aligned} \tag{50}$$

To determine the first unknown coefficient $\phi_1(\varkappa)$ in equation (46), we have to use 1st-truncated expansion $W_1(\varkappa, s) = 1/s \max(\varkappa - 25e^{-0.06}, 0) + \phi_1(\varkappa)/s^{\omega+1}$ into the 1st-LRF $\mathcal{L}[\text{Res}_1(\varkappa, s)]$, then we multiply by $s^{\omega+1}$ on both sides, and then we use the following fact $\lim_{s \rightarrow \infty} s^{\omega+1} \mathcal{L}[\text{Res}_1(\varkappa, s)] = 0$ to obtain

$$\phi_1(\varkappa) = -0.06[\varkappa - \max(\varkappa - 25e^{-0.06}, 0)]. \tag{51}$$

Similarly, to establish the value of the second undefined coefficient $\phi_2(\varkappa)$, we have to utilize the 2nd truncated expansion $W_2(\varkappa, s) = 1/s \max(\varkappa - 25e^{-0.06}, 0) + \phi_1(\varkappa)/s^{\omega+1} + \phi_2(\varkappa)/s^{2\omega+1}$ into the 2nd-LRF and use the following fact $\lim_{s \rightarrow \infty} s^{2\omega+1} \mathcal{L}[\text{Res}_2(\varkappa, s)] = 0$, we have

$$\phi_2(\varkappa) = -(0.06)^2 \varkappa - \max(\varkappa - 25e^{-0.06}, 0). \tag{52}$$

Therefore, the approximate solution derived from the 2nd iteration of equation (44) is as follows:

$$\begin{aligned} W_2(\varkappa, s) &= \frac{1}{s} (\max(\varkappa - 25e^{-0.06}, 0)) - \frac{0.06}{s^{\omega+1}} (\varkappa - \max(\varkappa - 25e^{-0.06}, 0)) \\ &\quad - \frac{(0.06)^2}{s^{2\omega+1}} (\varkappa - \max(\varkappa - 25e^{-0.06}, 0)). \end{aligned} \tag{53}$$

To determine the 3rd, 4th, and 5th unknown coefficients, we repeat the same process. We get as follows:

$$\begin{aligned} \phi_3(\kappa) &= -(0.06)^3(\kappa - \max(\kappa - 25e^{-0.06}, 0)), \\ \phi_4(\kappa) &= -(0.06)^4(\kappa - \max(\kappa - 25e^{-0.06}, 0)), \\ \phi_5(\kappa) &= -(0.06)^5(\kappa - \max(\kappa - 25e^{-0.06}, 0)). \end{aligned} \tag{54}$$

Therefore, the approximate solution derived from the 5th iteration of equation (44) is as follows:

$$W_5(\kappa, s) = \frac{1}{s}(\max(\kappa - 25e^{-0.06}, 0)) - \left[\frac{0.06}{s^{\varpi+1}} + \frac{(0.06)^2}{s^{2\varpi+1}} + \frac{(0.06)^3}{s^{3\varpi+1}} + \frac{(0.06)^4}{s^{4\varpi+1}} + \frac{(0.06)^5}{s^{5\varpi+1}} \right] (\kappa - \max(\kappa - 25e^{-0.06}, 0)). \tag{55}$$

By utilizing the inverse LT on both sides of equation (55), the approximate solution derived from the 5th iteration by LRPSM of equations (42) and (43) is as follows:

$$w_5(\kappa, \zeta) = \max(\kappa - 25e^{-0.06}, 0) - \left[\frac{(0.06\zeta^\varpi)}{\Gamma(\varpi + 1)} + \frac{(0.06\zeta^\varpi)^2}{\Gamma(2\varpi + 1)} + \frac{(0.06\zeta^\varpi)^3}{\Gamma(3\varpi + 1)} + \frac{(0.06\zeta^\varpi)^4}{\Gamma(4\varpi + 1)} + \frac{(0.06\zeta^\varpi)^5}{\Gamma(5\varpi + 1)} \right] (\kappa - \max(\kappa - 25e^{-0.06}, 0)). \tag{56}$$

When $\varpi = 1$ is used in equation (56), we get as follows:

$$w_5(\kappa, \zeta) = \max(\kappa - 25e^{-0.06}, 0) - \left[0.06\zeta + \frac{(0.06\zeta)^2}{2!} + \frac{(0.06\zeta)^3}{3!} + \frac{(0.06\zeta)^4}{4!} + \frac{(0.06\zeta)^5}{5!} \right] (\kappa - \max(\kappa - 25e^{-0.06}, 0)). \tag{57}$$

As a result, the following is the exact solution of equations (42) and (43) for $\varpi = 1$:

$$w(\kappa, \zeta) = \max(\kappa - 25e^{-0.06}, 0) + (1 - e^{0.06\zeta})(\kappa - \max(\kappa - 25e^{-0.06}, 0)). \tag{58}$$

subject to the initial condition:

$$w(\kappa, 0) = \max(e^\kappa - 1, 0). \tag{60}$$

First, we perform LT on both sides of equation (59), using the initial condition from equation (60), and then format the resulting equation as follows:

Problem 3. consider the following time-fractional BSOPE [36]:

$$\begin{aligned} \frac{\partial^\varpi w(\kappa, \zeta)}{\partial \zeta^\varpi} &= \frac{\partial^2 w(\kappa, \zeta)}{\partial \kappa^2} + (\lambda - 1) \frac{\partial w(\kappa, \zeta)}{\partial \kappa} \\ &\quad - \lambda w(\kappa, \zeta), \quad 0 < \varpi \leq 1, \end{aligned} \tag{59}$$

$$W(\kappa, s) = \frac{1}{s} \max(e^\kappa - 1, 0) + \frac{1}{s^\varpi} D_{\kappa\kappa} W(\kappa, s) + \frac{(\lambda - 1)}{s^\varpi} D_\kappa W(\kappa, s) - \frac{\lambda}{s^\varpi} W(\kappa, s). \tag{61}$$

We describe the expansion solution of the algebraic equation (61). Therefore, we assume that the expansion of $W(\varkappa, s)$ is as follows:

$$W(\varkappa, s) = \sum_{n=0}^{\infty} \frac{\phi_n(\varkappa)}{s^{n\omega+1}}. \tag{62}$$

The k th-truncated expansion of equation (61) is as follows:

$$W_k(\varkappa, s) = \frac{1}{s} \max(e^\varkappa - 1, 0) + \sum_{n=1}^k \frac{\phi_n(\varkappa)}{s^{n\omega+1}}. \tag{63}$$

The LRF of equation (61) takes the following form:

$$\mathcal{L}[\text{Res}(\varkappa, s)] = W(\varkappa, s) - \frac{1}{s} \max(e^\varkappa - 1, 0) - \frac{1}{s^\omega} D_{\varkappa x} W(\varkappa, s) - \frac{(\lambda - 1)}{s^\omega} D_x W(\varkappa, s) + \frac{\lambda}{s^\omega} W(\varkappa, s). \tag{64}$$

Accordingly, the k th-LRF takes the following form:

$$\mathcal{L}[\text{Res}_k(\varkappa, s)] = W_k(\varkappa, s) - \frac{1}{s} \max(e^\varkappa - 1, 0) - \frac{1}{s^\omega} D_{\varkappa x} W_k(\varkappa, s) - \frac{(\lambda - 1)}{s^\omega} D_x W_k(\varkappa, s) + \frac{\lambda}{s^\omega} W_k(\varkappa, s). \tag{65}$$

We substitute the k th-truncated series equations (63) into (64), multiply the resulting equation by $s^{k\omega+1}$, and then

solve the equation $\lim_{s \rightarrow \infty} s^{k\omega+1} \mathcal{L}[\text{Res}_k(\varkappa, s)] = 0$, where $k = 1, 2, 3, 4, 5$, for $\phi_k(\varkappa)$ gives

$$\begin{aligned} \phi_0(\varkappa, s) &= \max(e^\varkappa - 1, 0), \\ \phi_1(\varkappa, s) &= \lambda [\max(e^\varkappa, 0) - \max(e^\varkappa - 1, 0)], \\ \phi_2(\varkappa, s) &= -\lambda^2 [\max(e^\varkappa, 0) - \max(e^\varkappa - 1, 0)], \\ \phi_3(\varkappa, s) &= \lambda^3 [\max(e^\varkappa, 0) - \max(e^\varkappa - 1, 0)], \\ \phi_4(\varkappa, s) &= -\lambda^4 [\max(e^\varkappa, 0) - \max(e^\varkappa - 1, 0)], \\ \phi_5(\varkappa, s) &= \lambda^5 [\max(e^\varkappa, 0) - \max(e^\varkappa - 1, 0)]. \end{aligned} \tag{66}$$

Therefore, the approximate solution derived from the 5th iteration of equation (61) is as follows:

$$\begin{aligned} W_5(\varkappa, s) &= \frac{1}{s} \max(e^\varkappa - 1, 0) + \frac{\lambda}{s^{\omega+1}} [\max(e^\varkappa, 0) - \max(e^\varkappa - 1, 0)] - \frac{\lambda^2}{s^{2\omega+1}} [\max(e^\varkappa, 0) - \max(e^\varkappa - 1, 0)] \\ &+ \frac{\lambda^3}{s^{3\omega+1}} [\max(e^\varkappa, 0) - \max(e^\varkappa - 1, 0)] - \frac{\lambda^4}{s^{4\omega+1}} [\max(e^\varkappa, 0) - \max(e^\varkappa - 1, 0)] + \frac{\lambda^5}{s^{5\omega+1}} [\max(e^\varkappa, 0) - \max(e^\varkappa - 1, 0)]. \end{aligned} \tag{67}$$

By utilizing the inverse LT on both sides of equation (67), the approximate solution derived from the 5th iteration by LRPSM of equations (59) and (60) is as follows:

$$\begin{aligned}
w_5(\varkappa, \zeta) &= \max(e^\varkappa - 1, 0) + \frac{\lambda \zeta^\omega}{\Gamma(\omega + 1)} [\max(e^\varkappa, 0) - \max(e^\varkappa - 1, 0)] \\
&\quad - \frac{\lambda^2 \zeta^{2\omega}}{\Gamma(2\omega + 1)} [\max(e^\varkappa, 0) - \max(e^\varkappa - 1, 0)] + \frac{\lambda^3 \zeta^{3\omega}}{\Gamma(3\omega + 1)} [\max(e^\varkappa, 0) - \max(e^\varkappa - 1, 0)] \\
&\quad - \frac{\lambda^4 \zeta^{4\omega}}{\Gamma(4\omega + 1)} [\max(e^\varkappa, 0) - \max(e^\varkappa - 1, 0)] + \frac{\lambda^5 \zeta^{5\omega}}{\Gamma(5\omega + 1)} [\max(e^\varkappa, 0) - \max(e^\varkappa - 1, 0)].
\end{aligned} \tag{68}$$

When $\omega = 1$ is used in equation (68), we get as follows:

$$w_5(\varkappa, \zeta) = \max(e^\varkappa - 1, 0) + \left[\frac{\lambda \zeta}{1!} - \frac{\lambda^2 \zeta^2}{2!} + \frac{\lambda^3 \zeta^3}{3!} - \frac{\lambda^4 \zeta^4}{4!} + \frac{\lambda^5 \zeta^5}{5!} \right] [\max(e^\varkappa, 0) - \max(e^\varkappa - 1, 0)]. \tag{69}$$

As a result, the following is the exact solution of equations (59) and (60) for $\omega = 1$:

$$w(\varkappa, \zeta) = \max(e^\varkappa - 1, 0)e^{-\lambda \zeta} + \max(e^\varkappa, 0)(1 - e^{-\lambda \zeta}). \tag{70}$$

5. Numerical Simulation and Discussion

The findings of the results of the models presented in Problems 1–3 are evaluated graphically and numerically in this section. Error functions can be used to evaluate the numerical method's correctness and competency. It is important to provide the errors of the approximation analytical solution that the LRPSM offers in terms of an infinite fractional power series. We used the absolute and recurrence error functions to demonstrate the accuracy and strength of LRPSM.

The 2D graphs of the comparative analysis of the exact and approximative solutions derived by the suggested method in Problems 1–3 are shown in Figures 1(a)–1(c). These figures display the 2D plots of the precise solution and the approximate solution attained from the fifth iteration attained by LRPSM for Examples 1–3 when $\omega = 0.6, 0.7, 0.8, 0.9,$ and 1.0 in the range of $\zeta \in [0, 0.5]$. These graphs indicate that when $\omega \rightarrow 1.0$ is applied, the approximative solution converges to the precise solution. The precise result and the approximation overlap at $\omega = 1.0$, demonstrating the efficacy and accuracy of the recommended method.

Figures 2(a)–2(c) display the 2D curve of calculating the similarity with the help of absolute error of the approximation formed in the fifth step and the precise solution found by the suggested technique for Examples 1–3, respectively, for $\omega = 1.0$ in the range of $\zeta \in [0, 0.5]$. The article has shown that the fifth-step approximation solution of the recommended approach is very close to the exact solution. By showing the absolute error of the precise and approximate outputs on a graph, LRPSM's precision is proven.

The comparison article using the 3D curve is shown in Figures 3(a)–3(c) in the sense of the absolute error of the

approximate finding from the fifth iteration and the exact finding found using the suggested method to Examples 1–3, respectively, at $\omega = 1.0$ in the ranges of $\zeta \in [0, 0.2]$ and $\omega \in [0, 0.2]$. The article has revealed that the fifth-step approximation of the recommended approach is very similar to the precise result. The absolute error of the precise and approximation findings on 3D graphs serves as a demonstration of the precision of LRPSM.

In Tables 1–6, the numerical convergence of the approximation to the precise solution has been demonstrated by $|w^4(\varkappa, \zeta) - w^3(\varkappa, \zeta)|$ and $|w^5(\varkappa, \zeta) - w^4(\varkappa, \zeta)|$ in the range $\zeta \in [0, 0.1]$. Tables 1–6 shows that $w^4(\varkappa, \zeta)$ and $w^5(\varkappa, \zeta)$ obtained by the suggested method quickly approaches the $w(\varkappa, \zeta)$ when $\omega \rightarrow 1.0$. We can see from Tables 1, 3, and 5 that all of the test problems for the fourth stage have very low recurrence errors. The recurrence error will further decrease if we take into account the fifth-step approximation shown in Tables 2, 4, and 6. The approximation is rapidly approaching the exact solution as a result of the accuracy of our suggested strategy being demonstrated by the recurring error process. We arrived at the conclusion that the suggested approach is a feasible and efficient technique for solving particular classes of FODEs with fewer calculations and iteration steps.

For appropriately selected points, $|w(\varkappa, \zeta) - w^6(\varkappa, \zeta)|$ and $|w(\varkappa, \zeta) - w^7(\varkappa, \zeta)|$ in the range $\zeta \in [0, 0.1]$ obtained by LRPSM at $\omega = 1.0$ in Examples 1–3 are displayed in Tables 7–12 for comparison article in the sense of the absolute error of the approximate and the exact finding. We can see from Tables 7, 9, and 11 that approximate solutions derived from the 6th iteration for all of the test problems have very low errors. The absolute error will further decrease if we take into account the 7th-step approximation shown in Tables 8, 10, and 12. By quantitatively comparing the absolute inaccuracy of the precise and approximative findings, LRPSM's precision is shown.

Tables 13–15 also compares the absolute error of the approximations from the fifth iteration obtained by the LRPSM of Examples 1–3 at plausible short-listed grid points in the range $\zeta \in [0, 0.1]$ with the absolute error of the fifth-

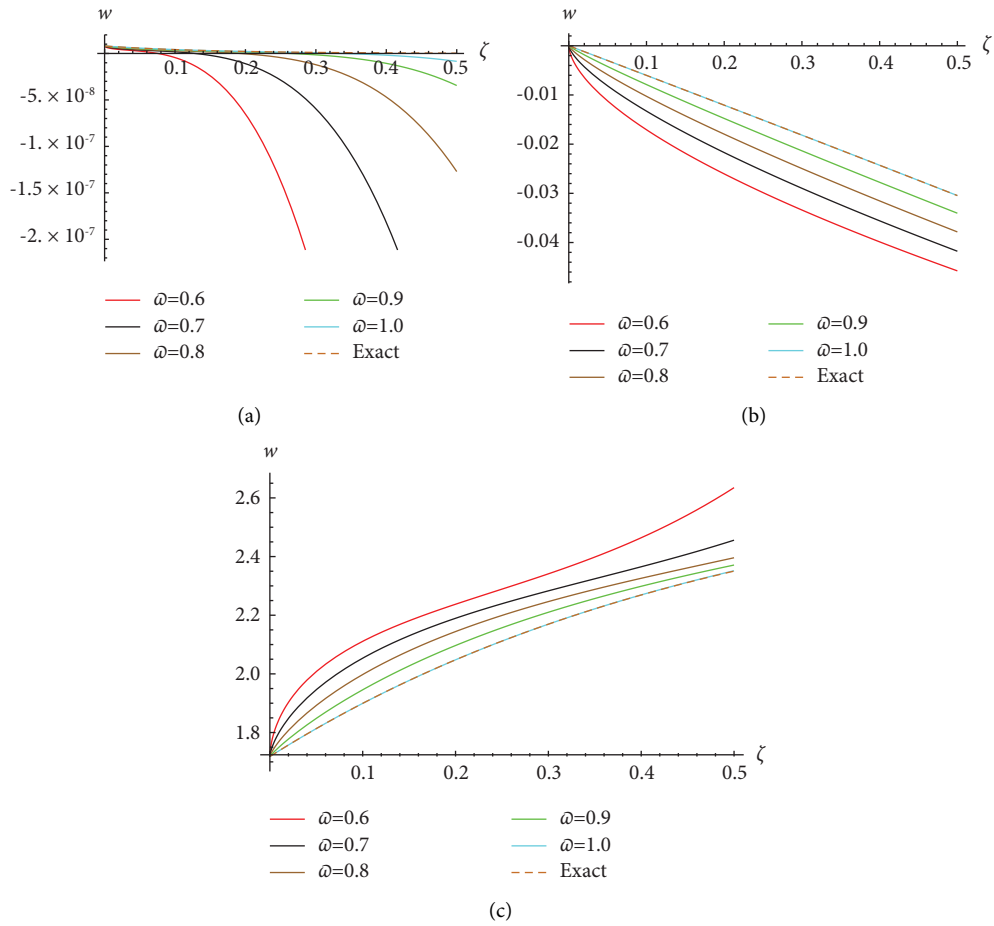


FIGURE 1: The approximate result of five iterations, as well as the exact result of $w(x, \zeta)$ for various values of ω in the range $\zeta \in [0, 0.5]$ for (a) Problem 1, when $\kappa = 0.002$, (b) Problem 2, when $\kappa = 1.0$, and (c) Problem 3, when $\kappa = 1.0$ and $\lambda = 2.0$.

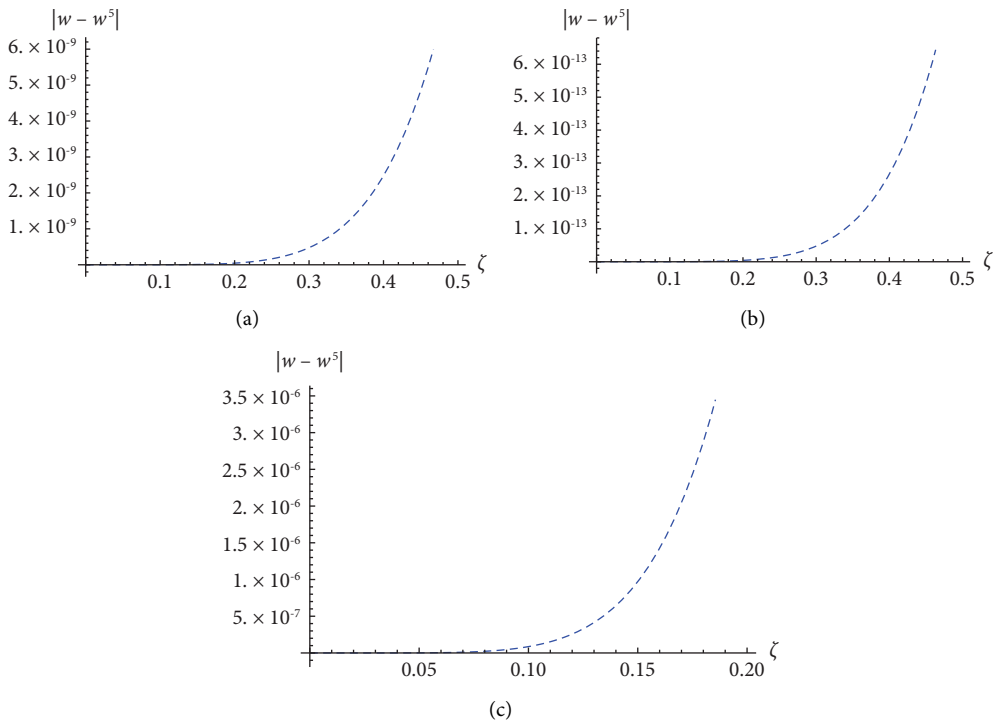


FIGURE 2: In Figure 2, the 2D curve of $|w(x, \zeta) - w^5(x, \zeta)|$ in the range $\zeta \in [0, 0.5]$, when $\omega = 1.0$ for (a) Problem 1, when $\kappa = 0.002$, (b) Problem 2, when $\kappa = 1.0$, and (c) Problem 3, when $\kappa = 1.0$ and $\lambda = 2.0$.

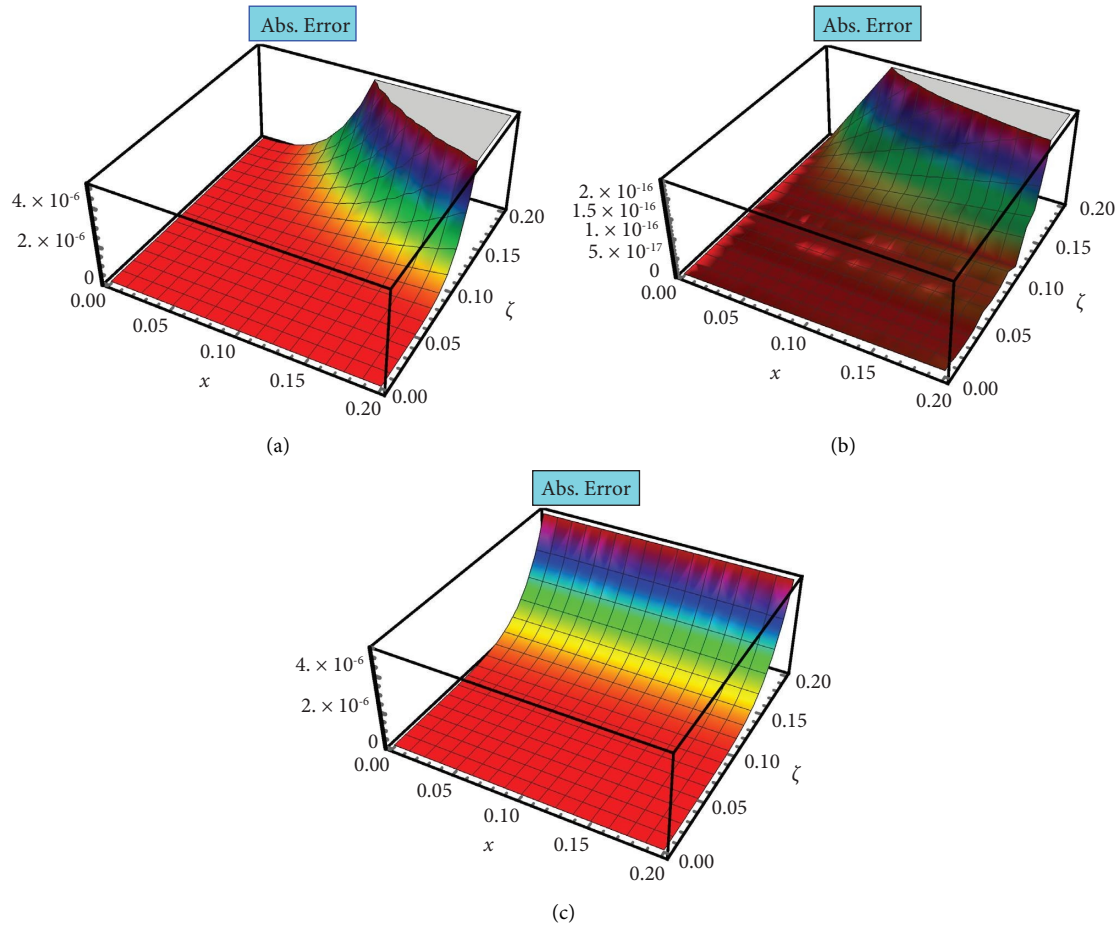


FIGURE 3: In Figure 3, the 3D curve of $|w(x, \zeta) - w^5(x, \zeta)|$ in the ranges $\zeta \in [0, 0.2]$ and $\varpi \in [0, 0.2]$, when $\varpi = 1.0$ for (a) Problem 1, (b) Problem 2, and (c) Problem 3, when $\lambda = 2.0$.

TABLE 1: $|w^4(x, \zeta) - w^3(x, \zeta)|$ of Problem 1 at different values of ϖ at $\kappa = 0.002$ determined by LRPSM at plausible locations in the range $\zeta \in [0, 0.1]$.

ζ	$\varpi = 0.7$	$\varpi = 0.8$	$\varpi = 0.9$	$\varpi = 1.0$
0.01	7.64160×10^{-12}	7.32938×10^{-13}	6.73357×10^{-14}	5.95021×10^{-15}
0.02	5.32192×10^{-11}	6.73539×10^{-12}	8.16495×10^{-13}	9.52033×10^{-14}
0.03	1.65624×10^{-10}	2.46522×10^{-11}	3.51465×10^{-12}	4.81967×10^{-13}
0.04	3.70640×10^{-10}	6.18955×10^{-11}	9.90060×10^{-12}	1.52325×10^{-12}
0.05	6.92309×10^{-10}	1.26407×10^{-10}	2.21074×10^{-11}	3.71888×10^{-12}
0.06	1.15347×10^{-9}	2.26543×10^{-10}	4.26177×10^{-11}	7.71147×10^{-12}
0.07	1.77606×10^{-9}	3.71006×10^{-10}	7.42333×10^{-11}	1.42865×10^{-11}
0.08	2.58129×10^{-9}	5.68794×10^{-10}	1.20052×10^{-10}	2.43721×10^{-11}
0.09	3.58974×10^{-9}	8.29169×10^{-10}	1.83450×10^{-10}	3.90393×10^{-11}
0.1	4.82152×10^{-9}	1.84106×10^{-10}	3.37478×10^{-11}	5.95021×10^{-12}

TABLE 2: $|w^5(x, \zeta) - w^4(x, \zeta)|$ of Problem 1 at different values of ϖ at $\kappa = 0.002$ determined by LRPSM at plausible locations in the range $\zeta \in [0, 0.1]$.

ζ	$\varpi = 0.7$	$\varpi = 0.8$	$\varpi = 0.9$	$\varpi = 1.0$
0.01	7.98018×10^{-13}	3.86764×10^{-14}	1.77337×10^{-15}	7.73527×10^{-17}
0.02	9.02854×10^{-12}	6.18822×10^{-13}	4.01268×10^{-14}	2.47529×10^{-15}
0.03	3.73196×10^{-11}	3.13278×10^{-12}	2.48797×10^{-13}	1.87967×10^{-14}
0.04	1.02146×10^{-10}	9.90115×10^{-12}	9.07967×10^{-13}	7.92092×10^{-14}
0.05	2.23053×10^{-10}	2.41727×10^{-11}	2.47836×10^{-12}	2.41727×10^{-13}
0.06	4.22223×10^{-10}	5.01246×10^{-11}	5.62964×10^{-12}	6.01495×10^{-13}
0.07	7.24195×10^{-10}	9.28619×10^{-11}	1.12653×10^{-11}	1.30007×10^{-12}
0.08	1.15565×10^{-9}	1.58418×10^{-10}	2.05449×10^{-11}	2.53469×10^{-12}
0.09	1.74526×10^{-9}	2.53756×10^{-10}	3.49053×10^{-11}	4.56760×10^{-12}
0.1	2.52355×10^{-9}	3.86764×10^{-10}	5.60790×10^{-11}	7.73527×10^{-12}

TABLE 3: $|w^4(\kappa, \zeta) - w^3(\kappa, \zeta)|$ of Problem 2 at different values of ϖ at $\kappa = 1.0$ determined by LRPSM at plausible locations in the range $\zeta \in [0, 0.1]$.

ζ	$\varpi = 0.7$	$\varpi = 0.8$	$\varpi = 0.9$	$\varpi = 1.0$
0.01	6.93499×10^{-12}	6.65164×10^{-13}	6.11093×10^{-14}	5.40000×10^{-15}
0.02	4.82981×10^{-11}	6.11258×10^{-12}	7.40995×10^{-13}	8.64000×10^{-14}
0.03	1.50309×10^{-10}	2.23726×10^{-11}	3.18965×10^{-12}	4.37400×10^{-13}
0.04	3.36367×10^{-10}	5.61721×10^{-11}	8.98510×10^{-12}	1.38240×10^{-12}
0.05	6.28292×10^{-10}	1.14718×10^{-10}	2.00632×10^{-11}	3.37500×10^{-12}
0.06	1.04681×10^{-9}	2.05595×10^{-10}	3.86769×10^{-11}	6.99840×10^{-12}
0.07	1.61183×10^{-9}	3.36699×10^{-10}	6.73690×10^{-11}	1.29654×10^{-11}
0.08	2.34260×10^{-9}	5.16198×10^{-10}	1.08951×10^{-10}	2.21184×10^{-11}
0.09	3.25780×10^{-9}	7.52497×10^{-10}	2.50264×10^{-9}	3.54294×10^{-11}
0.1	4.37568×10^{-9}	1.05421×10^{-9}	2.43280×10^{-10}	5.40000×10^{-11}

TABLE 4: $|w^5(\kappa, \zeta) - w^4(\kappa, \zeta)|$ of Problem 2 at different values of ϖ at $\kappa = 1.0$ determined by LRPSM at plausible locations in the range $\zeta \in [0, 0.1]$.

ζ	$\varpi = 0.7$	$\varpi = 0.8$	$\varpi = 0.9$	$\varpi = 1.0$
0.01	6.68516×10^{-15}	3.24000×10^{-16}	1.48559×10^{-17}	6.48000×10^{-19}
0.02	7.56340×10^{-14}	5.18400×10^{-15}	3.36151×10^{-16}	2.07360×10^{-17}
0.03	3.12634×10^{-13}	2.62440×10^{-14}	2.08423×10^{-15}	1.57464×10^{-16}
0.04	8.55701×10^{-13}	8.29440×10^{-14}	7.60623×10^{-15}	6.63552×10^{-16}
0.05	1.86856×10^{-12}	2.02500×10^{-13}	2.07618×10^{-14}	2.02500×10^{-15}
0.06	3.53705×10^{-12}	4.19904×10^{-13}	4.71607×10^{-14}	5.03885×10^{-15}
0.07	6.06674×10^{-12}	7.77924×10^{-13}	9.43715×10^{-14}	1.08909×10^{-14}
0.08	9.68115×10^{-12}	1.32710×10^{-12}	1.72109×10^{-13}	2.12337×10^{-14}
0.09	1.46205×10^{-11}	2.12576×10^{-12}	2.92409×10^{-13}	3.82638×10^{-14}
0.1	2.11403×10^{-11}	3.24000×10^{-12}	4.69785×10^{-13}	6.48000×10^{-14}

TABLE 5: $|w^4(\kappa, \zeta) - w^3(\kappa, \zeta)|$ of Problem 3 at different values of ϖ at $\kappa = 0.002$ when $\lambda = 2.0$ determined by LRPSM at plausible locations in the range $\zeta \in [0, 0.1]$.

ζ	$\varpi = 0.7$	$\varpi = 0.8$	$\varpi = 0.9$	$\varpi = 1.0$
0.01	1.71234×10^{-5}	1.64238×10^{-6}	1.50887×10^{-7}	1.33333×10^{-8}
0.02	1.19254×10^{-4}	1.5092810×10^{-5}	1.82962×10^{-6}	2.13333×10^{-7}
0.03	3.71134×10^{-4}	5.52410×10^{-5}	7.87569×10^{-6}	1.08000×10^{-6}
0.04	8.30537×10^{-4}	1.38697×10^{-4}	2.21854×10^{-5}	3.41333×10^{-6}
0.05	1.55134×10^{-3}	2.83255×10^{-4}	4.95386×10^{-5}	8.33333×10^{-6}
0.06	2.58472×10^{-3}	5.07642×10^{-4}	9.54985×10^{-5}	1.72800×10^{-5}
0.07	3.97984×10^{-3}	8.31357×10^{-4}	1.66343×10^{-4}	3.20133×10^{-5}
0.08	5.78419×10^{-3}	1.27456×10^{-3}	2.69015×10^{-4}	5.46133×10^{-5}
0.09	8.04396×10^{-3}	1.85802×10^{-3}	4.11079×10^{-4}	8.74800×10^{-5}
0.1	1.08042×10^{-2}	2.60300×10^{-3}	6.00692×10^{-4}	1.33333×10^{-4}

TABLE 6: $|w^5(\kappa, \zeta) - w^4(\kappa, \zeta)|$ of Problem 3 at different values of ϖ at $\kappa = 0.002$ when $\lambda = 2.0$ determined by LRPSM at plausible locations in the range $\zeta \in [0, 0.1]$.

ζ	$\varpi = 0.7$	$\varpi = 0.8$	$\varpi = 0.9$	$\varpi = 1.0$
0.01	2.75110×10^{-7}	1.33333×10^{-8}	6.11355×10^{-10}	2.66667×10^{-11}
0.02	3.11251×10^{-6}	2.13333×10^{-7}	1.38334×10^{-8}	8.53333×10^{-10}
0.03	1.28656×10^{-5}	1.08000×10^{-6}	8.57707×10^{-8}	6.48000×10^{-9}
0.04	3.52140×10^{-5}	3.41333×10^{-6}	3.13014×10^{-7}	2.73067×10^{-8}
0.05	7.68955×10^{-5}	8.33333×10^{-6}	8.54394×10^{-7}	8.33333×10^{-8}
0.06	1.45558×10^{-4}	1.72800×10^{-5}	1.94077×10^{-6}	2.07360×10^{-7}
0.07	2.49660×10^{-4}	3.20133×10^{-5}	3.88360×10^{-6}	4.48187×10^{-7}
0.08	3.98401×10^{-4}	5.46133×10^{-5}	7.08269×10^{-6}	8.73813×10^{-7}
0.09	6.01665×10^{-4}	8.74800×10^{-5}	1.20333×10^{-5}	1.57464×10^{-6}
0.1	8.69973×10^{-4}	1.33333×10^{-4}	1.93327×10^{-5}	2.66667×10^{-6}

TABLE 7: $|w(\kappa, \zeta) - w^6(\kappa, \zeta)|$ of Problem 1 at $\kappa = 0.003$ when $\varpi = 1.0$ determined by LRPSM at plausible locations in the range $\zeta \in [0, 0.1]$.

ζ	$w(\kappa, \zeta)$	$w^6(\kappa, \zeta)$	$ w^6(\kappa, \zeta) - w(\kappa, \zeta) $
0.01	2.53008×10^{-8}	2.53008×10^{-8}	2.60496×10^{-20}
0.02	2.37086×10^{-8}	2.37086×10^{-8}	3.30768×10^{-18}
0.03	2.22165×10^{-8}	2.22165×10^{-8}	5.60646×10^{-17}
0.04	2.08184×10^{-8}	2.08184×10^{-8}	4.16685×10^{-16}
0.05	1.95082×10^{-8}	1.95082×10^{-8}	1.97128×10^{-15}
0.06	1.82805×10^{-8}	1.82805×10^{-8}	7.00821×10^{-15}
0.07	1.71301×10^{-8}	1.71301×10^{-8}	2.04572×10^{-14}
0.08	1.60521×10^{-8}	1.60521×10^{-8}	5.16919×10^{-14}
0.09	1.50419×10^{-8}	1.50420×10^{-8}	1.16989×10^{-13}
0.1	1.40952×10^{-8}	1.40955×10^{-8}	2.42728×10^{-13}

TABLE 8: $|w(\kappa, \zeta) - w^7(\kappa, \zeta)|$ of Problem 1 at $\kappa = 0.003$ when $\varpi = 1.0$ determined by LRPSM at plausible locations in the range $\zeta \in [0, 0.1]$.

ζ	$w(\kappa, \zeta)$	$w^7(\kappa, \zeta)$	$ w(\kappa, \zeta) - w^7(\kappa, \zeta) $
0.01	2.53008×10^{-8}	2.53008×10^{-8}	2.11758×10^{-22}
0.02	2.37086×10^{-8}	2.37086×10^{-8}	5.38461×10^{-20}
0.03	2.22165×10^{-8}	2.22165×10^{-8}	1.37022×10^{-18}
0.04	2.08184×10^{-8}	2.08184×10^{-8}	1.35902×10^{-17}
0.05	1.95082×10^{-8}	1.95082×10^{-8}	8.0436×10^{-17}
0.06	1.82805×10^{-8}	1.82805×10^{-8}	3.43448×10^{-16}
0.07	1.71301×10^{-8}	1.71301×10^{-8}	1.17061×10^{-15}
0.08	1.60521×10^{-8}	1.60521×10^{-8}	3.38332×10^{-15}
0.09	1.50419×10^{-8}	1.50418×10^{-8}	8.62135×10^{-15}
0.1	1.40952×10^{-8}	1.40952×10^{-8}	1.98913×10^{-14}

TABLE 9: $|w(\kappa, \zeta) - w^6(\kappa, \zeta)|$ of Problem 2 at $\kappa = 1.0$ when $\varpi = 1.0$ determined by LRPSM at plausible locations in the range $\zeta \in [0, 0.1]$.

ζ	$w(\kappa, \zeta)$	$w^6(\kappa, \zeta)$	$ w(\kappa, \zeta) - w^6(\kappa, \zeta) $
0.01	-0.00060018	-0.00060018	2.95987×10^{-17}
0.02	-0.00120072	-0.00120072	4.42354×10^{-17}
0.03	-0.00180162	-0.00180162	7.69784×10^{-17}
0.04	-0.00240288	-0.00240288	7.19910×10^{-17}
0.05	-0.00300450	-0.00300450	5.46438×10^{-17}
0.06	-0.00360649	-0.00360649	1.00614×10^{-16}
0.07	-0.00420883	-0.00420883	5.72459×10^{-17}
0.08	-0.00481154	-0.00481154	3.12250×10^{-17}
0.09	-0.00541461	-0.00541461	7.28584×10^{-17}
0.1	-0.00601804	-0.00601804	5.89806×10^{-17}

TABLE 10: $|w(\kappa, \zeta) - w^7(\kappa, \zeta)|$ of Problem 2 at $\kappa = 1.0$ when $\varpi = 1.0$ determined by LRPSM at plausible locations in the range $\zeta \in [0, 0.1]$.

ζ	$w(\kappa, \zeta)$	$w^7(\kappa, \zeta)$	$ w(\kappa, \zeta) - w^7(\kappa, \zeta) $
0.01	-0.00060018	-0.00060018	2.94903×10^{-17}
0.02	-0.00120072	-0.00120072	4.40186×10^{-17}
0.03	-0.00180162	-0.00180162	7.67615×10^{-17}
0.04	-0.00240288	-0.00240288	7.15573×10^{-17}
0.05	-0.00300450	-0.00300450	5.50775×10^{-17}
0.06	-0.00360649	-0.00360649	1.00614×10^{-16}
0.07	-0.00420883	-0.00420883	5.63785×10^{-17}
0.08	-0.00481154	-0.00481154	3.12250×10^{-17}
0.09	-0.00541461	-0.00541461	7.28584×10^{-17}
0.1	-0.00601804	-0.00601804	5.89806×10^{-17}

TABLE 11: $|w(\varkappa, \zeta) - w^6(\varkappa, \zeta)|$ of Problem 3 at $\varkappa = 1.0$ and $\lambda = 2.0$ when $\varpi = 1.0$ determined by LRPSM at plausible locations in the range $\zeta \in [0, 0.1]$.

ζ	$w(\varkappa, \zeta)$	$w^6(\varkappa, \zeta)$	$ w(\varkappa, \zeta) - w^6(\varkappa, \zeta) $
0.01	1.73808	1.73808	2.22045×10^{-16}
0.02	1.75749	1.75749	3.24185×10^{-14}
0.03	1.77652	1.77652	5.51115×10^{-13}
0.04	1.79517	1.79517	4.11982×10^{-12}
0.05	1.81344	1.81344	1.95961×10^{-11}
0.06	1.83136	1.83136	7.00426×10^{-11}
0.07	1.84892	1.84892	2.05550×10^{-10}
0.08	1.86614	1.86614	5.22144×10^{-10}
0.09	1.88301	1.88301	1.18793×10^{-9}
0.1	1.73808	1.89955	2.47757×10^{-9}

TABLE 12: $|w(\varkappa, \zeta) - w^7(\varkappa, \zeta)|$ of Problem 3 at $\varkappa = 1.0$ and $\lambda = 2.0$ when $\varpi = 1.0$ determined by LRPSM at plausible locations in the range $\zeta \in [0, 0.1]$.

ζ	$w(\varkappa, \zeta)$	$w^7(\varkappa, \zeta)$	$ w(\varkappa, \zeta) - w^7(\varkappa, \zeta) $
0.01	1.73808	1.73808	0.0
0.02	1.75749	1.75749	0.0
0.03	1.77652	1.77652	4.21885×10^{-15}
0.04	1.79517	1.79517	4.10783×10^{-14}
0.05	1.81344	1.81344	2.45359×10^{-13}
0.06	1.83136	1.83136	1.05249×10^{-12}
0.07	1.84892	1.84892	3.60423×10^{-12}
0.08	1.86614	1.86614	1.04659×10^{-11}
0.09	1.88301	1.88301	2.67941×10^{-11}
0.1	1.73808	1.89955	6.21085×10^{-11}

TABLE 13: $|w(\varkappa, \zeta) - w^5(\varkappa, \zeta)|$ in different approaches for Problem 1 at $\varkappa = 0.002$ when $\varpi = 1.0$ at plausible locations in the range $\zeta \in [0, 0.1]$.

ζ	Abs.error [LRPSM]	Abs.error [PDTM] [34]
0.01	8.30269×10^{-19}	8.30269×10^{-19}
0.02	5.26512×10^{-17}	5.26512×10^{-17}
0.03	5.94281×10^{-16}	5.94281×10^{-16}
0.04	3.30894×10^{-15}	3.30894×10^{-15}
0.05	1.25095×10^{-14}	1.25095×10^{-14}
0.06	3.70206×10^{-14}	3.70206×10^{-14}
0.07	9.25270×10^{-14}	9.25270×10^{-14}
0.08	2.04357×10^{-13}	2.04357×10^{-13}
0.09	4.10678×10^{-13}	4.10678×10^{-13}
0.1	7.66068×10^{-13}	7.66068×10^{-13}

TABLE 14: $|w(\varkappa, \zeta) - w^5(\varkappa, \zeta)|$ in different approaches for Problem 2 at $\varkappa = 1.0$ when $\varpi = 1.0$ at plausible locations in the range $\zeta \in [0, 0.1]$.

ζ	Abs.error [LRPSM]	Abs.error [ATDM] [35]
0.01	2.94903×10^{-17}	2.94903×10^{-17}
0.02	4.40186×10^{-17}	4.40186×10^{-17}
0.03	7.67615×10^{-17}	7.67615×10^{-17}
0.04	7.11237×10^{-17}	7.11237×10^{-17}
0.05	5.63785×10^{-17}	5.63785×10^{-17}
0.06	1.03216×10^{-16}	1.03216×10^{-16}
0.07	6.41848×10^{-17}	6.41848×10^{-17}
0.08	1.47451×10^{-17}	1.47451×10^{-17}
0.09	1.07553×10^{-16}	1.07553×10^{-16}
0.1	1.23165×10^{-16}	1.23165×10^{-16}

TABLE 15: $|w(\kappa, \zeta) - w^s(\kappa, \zeta)|$ in different approaches for Problem 3 at $\kappa = 1.0$ and $\lambda = 2.0$ when $\varpi = 1.0$ at plausible locations in the range $\zeta \in [0, 0.1]$.

ζ	Abs.error [LRPSM]	Abs.error [HPM] [36]
0.01	8.88178×10^{-14}	8.88178×10^{-14}
0.02	5.65636×10^{-12}	5.65636×10^{-12}
0.03	6.42488×10^{-11}	6.42488×10^{-11}
0.04	3.59969×10^{-10}	3.59969×10^{-10}
0.05	1.36929×10^{-9}	1.36929×10^{-9}
0.06	4.07716×10^{-9}	4.07716×10^{-9}
0.07	1.02521×10^{-8}	1.02521×10^{-8}
0.08	2.27795×10^{-8}	2.27795×10^{-8}
0.09	4.60513×10^{-8}	4.60513×10^{-8}
0.1	8.64113×10^{-8}	8.64113×10^{-8}

step approximations obtained by various methods, including the PDTM [34], ATDM [35], and HPM [36]. Strong agreement between the results produced using the suggested method and various series solution techniques shows that the LRPSM is a useful substitute for approaches based on He's or Adomian polynomials.

6. Conclusion

In this article, we used the LRPSM to solve time-fractional BSOPE in the sense of CD. The effectiveness of the LRPSM has been demonstrated by results in both graphs and numerically. The approximate solutions achieved using LRPSM are in perfect agreement with the corresponding exact solutions, as can be seen from the graphs and tables. The numerical evidence for the convergence of the approximate solution to the exact solution is presented in Tables 1–6. The comparison article is established in Tables 7–12 in terms of the absolute error of the approximate and exact solutions. The results of these numerical approaches are also compared with the PDTM, ATDM, and HPM in terms of absolute errors in Tables 13–15.

The results obtained using the suggested approach, which demonstrates excellent agreement with PDTM, ATDM, and HPM, show that LRPSM is a suitable replacement tool for He's or Adomian polynomial-based methods used to solve FODEs. When determining the coefficients for a series such as the RPSM, the fractional derivative needs to be determined each time. However, LRPSM just needs the idea of an infinite limit. As a result, the computations required to determine the coefficients are minimal. The results led us to the conclusion that our technique is easy to use, accurate, flexible, and effective.

Data Availability

No data were generated or analyzed during the current study.

Conflicts of Interest

The authors declare that they have no conflicts of interest.

Authors' Contributions

The authors declare that the study was realized in collaboration with equal responsibility. All authors read and approved the final manuscript.

References

- [1] V. V. Kulish and J. L. Lage, "Application of fractional calculus to fluid mechanics," *Journal of Fluids Engineering*, vol. 124, no. 3, pp. 803–806, 2002.
- [2] V. E. Tarasov, "On history of mathematical economics: application of fractional calculus," *Mathematics*, vol. 7, no. 6, p. 509, 2019.
- [3] H. Sun, Y. Zhang, D. Baleanu, W. Chen, and Y. Chen, "A new collection of real world applications of fractional calculus in science and engineering," *Communications in Nonlinear Science and Numerical Simulation*, vol. 64, pp. 213–231, 2018.
- [4] Y. A. Rossikhin and M. V. Shitikova, "Application of fractional calculus for dynamic problems of solid mechanics: novel trends and recent results," *Applied Mechanics Reviews*, vol. 63, no. 1, 2010.
- [5] D. Valério, J. T. Machado, and V. Kiryakova, "Some pioneers of the applications of fractional calculus," *Fractional Calculus and Applied Analysis*, vol. 17, no. 2, pp. 552–578, 2014.
- [6] S. Rezapour, M. I. Liaqat, and S. Etemad, "An effective new iterative method to solve conformable Cauchy reaction-diffusion equation via the Shehu transform," *Journal of Mathematics*, vol. 2022, Article ID 4172218, 12 pages, 2022.
- [7] E. Bas and R. Ozarslan, "Real world applications of fractional models by Atangana-Baleanu fractional derivative," *Chaos, Solitons & Fractals*, vol. 116, pp. 121–125, 2018.
- [8] M. I. Liaqat, A. Khan, A. Akgül, and M. Ali, "A novel numerical technique for fractional ordinary differential equations with proportional delay," *Journal of Function Spaces*, vol. 2022, Article ID 6333084, 21 pages, 2022.
- [9] A. Traore and N. Sene, "Model of economic growth in the context of fractional derivative," *Alexandria Engineering Journal*, vol. 59, no. 6, pp. 4843–4850, 2020.
- [10] A. Khan, M. I. Liaqat, M. Younis, and A. Alam, "Approximate and exact solutions to fractional order Cauchy reaction-diffusion equations by new combine techniques," *Journal of Mathematics*, vol. 2021, Article ID 5337255, 12 pages, 2021.
- [11] R. Hilfer, Y. Luchko, and Z. Tomovski, "Operational method for the solution of fractional differential equations with

- generalized Riemann-Liouville fractional derivatives,” *Fractional Calculus and Applied Analysis*, vol. 12, no. 3, pp. 299–318, 2009.
- [12] M. I. Liaqat and E. Okyere, “The fractional series solutions for the conformable time-fractional swift-hohenberg equation through the conformable shehu daftardar-jafari approach with comparative analysis,” *Journal of Mathematics*, vol. 2022, Article ID 3295076, 20 pages, 2022.
- [13] M. I. Liaqat, A. Khan, M. Alam, M. K. Pandit, S. Etemad, and S. Rezapour, “Approximate and closed-form solutions of Newell-Whitehead-Segel equations via modified conformable Shehu transform decomposition method,” *Mathematical Problems in Engineering*, vol. 2022, Article ID 6752455, 14 pages, 2022.
- [14] B. J. Gireesha and G. Sowmya, “Heat transfer analysis of an inclined porous fin using Differential Transform Method,” *International Journal of Ambient Energy*, vol. 43, no. 1, pp. 3189–3195, 2022.
- [15] M. Nadeem, F. Li, and H. Ahmad, “Modified Laplace variational iteration method for solving fourth-order parabolic partial differential equation with variable coefficients,” *Computers & Mathematics with Applications*, vol. 78, no. 6, pp. 2052–2062, 2019.
- [16] S. M. Aznam and M. S. H. Chowdhury, “Generalized Haar wavelet operational matrix method for solving hyperbolic heat conduction in thin surface layers,” *Results in Physics*, vol. 11, pp. 243–252, 2018.
- [17] P. A. Naik, J. Zu, and M. Ghoreishi, “Estimating the approximate analytical solution of HIV viral dynamic model by using homotopy analysis method,” *Chaos, Solitons & Fractals*, vol. 131, Article ID 109500, 2020.
- [18] M. I. Liaqat, A. Khan, M. Alam, and M. K. Pandit, “A highly accurate technique to obtain exact solutions to time-fractional quantum mechanics problems with zero and nonzero trapping potential,” *Journal of Mathematics*, vol. 2022, Article ID 9999070, 20 pages, 2022.
- [19] D. Baleanu, S. Zibaei, M. Namjoo, and A. Jajarmi, “A non-standard finite difference scheme for the modeling and nonidentical synchronization of a novel fractional chaotic system,” *Advances in Difference Equations*, vol. 2021, no. 1, pp. 1–19, 2021.
- [20] M. I. Liaqat, A. Khan, and A. Akgül, “Adaptation on power series method with conformable operator for solving fractional order systems of nonlinear partial differential equations,” *Chaos, Solitons & Fractals*, vol. 157, Article ID 111984, 2022.
- [21] W. Xiang, S. Yan, J. Wu, and W. Niu, “Dynamic response and sensitivity analysis for mechanical systems with clearance joints and parameter uncertainties using Chebyshev polynomials method,” *Mechanical Systems and Signal Processing*, vol. 138, Article ID 106596, 2020.
- [22] O. Abu Arqub, “Application of residual power series method for the solution of time-fractional Schrödinger equations in one-dimensional space,” *Fundamenta Informaticae*, vol. 166, no. 2, pp. 87–110, 2019.
- [23] M. I. Liaqat and A. Akgül, “A novel approach for solving linear and nonlinear time-fractional Schrödinger equations,” *Chaos, Solitons & Fractals*, vol. 162, Article ID 112487, 2022.
- [24] T. Eriqat, A. El-Ajou, N. O. Moa’ath, Z. Al-Zhour, and S. Momani, “A new attractive analytic approach for solutions of linear and nonlinear neutral fractional pantograph equations,” *Chaos, Solitons & Fractals*, vol. 138, Article ID 109957, 2020.
- [25] M. Alaroud, “Application of Laplace residual power series method for approximate solutions of fractional IVP’s,” *Alexandria Engineering Journal*, vol. 61, no. 2, pp. 1585–1595, 2022.
- [26] M. Alquran, M. Ali, M. Alsukhour, and I. Jaradat, “Promoted residual power series technique with Laplace transform to solve some time-fractional problems arising in physics,” *Results in Physics*, vol. 19, Article ID 103667, 2020.
- [27] M. A. N. Oqielat, T. Eriqat, Z. Al-Zhour, O. Ogilat, and A. El-Ajou, I. Hashim, “Construction of fractional series solutions to nonlinear fractional reaction diffusion for bacteria growth model via Laplace residual power series method,” *International Journal of Dynamics and Control*, pp. 1–8, 2022.
- [28] H. Aljarrah, M. Alaroud, A. Ishak, and M. Darus, “Approximate solution of nonlinear time-fractional PDEs by Laplace residual power series method,” *Mathematics*, vol. 10, no. 12, p. 1980, 2022.
- [29] R. Saadeh, A. Burqan, and A. El-Ajou, “Reliable solutions to fractional Lane-Emden equations via Laplace transform and residual error function,” *Alexandria Engineering Journal*, vol. 61, no. 12, pp. 10551–10562, 2022.
- [30] S. M. Nuugulu, F. Gideon, and K. C. Patidar, “A robust numerical solution to a time-fractional Black-Scholes equation,” *Advances in Difference Equations*, vol. 2021, no. 1, pp. 1–25, 2021.
- [31] R. H. De Staelen and A. S. Hendy, “Numerically pricing double barrier options in a time-fractional Black-Scholes model,” *Computers & Mathematics with Applications*, vol. 74, no. 6, pp. 1166–1175, 2017.
- [32] V. P. Dubey, R. Kumar, and D. Kumar, “A reliable treatment of residual power series method for time-fractional Black-Scholes European option pricing equations,” *Physica A: Statistical Mechanics and Its Applications*, vol. 533, Article ID 122040, 2019.
- [33] M. Yavuz and N. Özdemiř, “A different approach to the European option pricing model with new fractional operator,” *Mathematical Modelling of Natural Phenomena*, vol. 13, no. 1, p. 12, 2018.
- [34] S. O. Edeki, O. O. Ugbebor, and E. A. Owoloko, “Analytical solution of the time-fractional order Black-Scholes model for stock option valuation on no dividend yield basis,” *IAENG International Journal of Applied Mathematics*, vol. 47, no. 4, pp. 1–10, 2017.
- [35] S. Alfaqeh and T. Ozis, “Solving fractional Black-Scholes European option pricing equations by Aboodh transform Decomposition method,” *Palestine Journal of Mathematics*, vol. 9, no. 2, pp. 915–924, 2020.
- [36] S. Kumar, D. Kumar, and J. Singh, “Numerical computation of fractional Black-Scholes equation arising in financial market,” *Egyptian Journal of Basic and Applied Sciences*, vol. 1, no. 3-4, pp. 177–183, 2014.
- [37] M. A. M. Ghandehari and M. Ranjbar, “European option pricing of fractional Black-Scholes model with new Lagrange multipliers,” *Computational Methods for Differential Equations*, vol. 2, no. 1, pp. 1–10, 2014.
- [38] S. O. Edeki, R. M. Jena, S. Chakraverty, and D. Baleanu, “Coupled transform method for time-space fractional Black-Scholes option pricing model,” *Alexandria Engineering Journal*, vol. 59, no. 5, pp. 3239–3246, 2020.
- [39] M. A. M. Ghandehari and M. Ranjbar, “European option pricing of fractional version of the Black-Scholes model: approach via expansion in series,” *International Journal of Nonlinear Science*, vol. 17, no. 2, pp. 105–110, 2014.

- [40] A. R. Kanth and K. Aruna, "Solution of time fractional Black-Scholes European option pricing equation arising in financial market," *Nonlinear Engineering*, vol. 5, no. 4, pp. 269–276, 2016.
- [41] M. I. Liaqat, S. Etemad, S. Rezapour, and C. Park, "A novel analytical Aboodh residual power series method for solving linear and nonlinear time-fractional partial differential equations with variable coefficients," *AIMS Mathematics*, vol. 7, no. 9, pp. 16917–16948, 2022.
- [42] M. Alquran, "Analytical solutions of fractional foam drainage equation by residual power series method," *Mathematical sciences*, vol. 8, no. 4, pp. 153–160, 2014.
- [43] D. G. Prakasha, P. Veerasha, and H. M. Baskonus, "Residual power series method for fractional Swift-Hohenberg equation," *Fractal and fractional*, vol. 3, no. 1, p. 9, 2019.